Neuropsychopharmacology (2015) 40, 1928–1939

www.neuropsychopharmacology.org

KCNN Genes that Encode Small-Conductance Ca^{2+}-Activated K^+ Channels Influence Alcohol and Drug Addiction

Audrey E Padula[1], William C Griffin III[1], Marcelo F Lopez[1], Sudarat Nimitvilai[1], Reginald Cannady[1], Natalie S McGuier[1], Elissa J Chesler[2], Michael F Miles[3], Robert W Williams[4], Patrick K Randall[1], John J Woodward[1], Howard C Becker[1] and Patrick J Mulholland*[,1]

[1]Department of Neuroscience, Medical University of South Carolina, Charleston, SC, USA; [2]The Jackson Laboratory, Bar Harbor, Maine, USA; [3]Virginia Commonwealth University, Richmond, VA, USA; [4]University of Tennessee Health Sciences Center, Memphis, TN, USA

Small-conductance Ca^{2+}-activated K^+ ($K_{Ca}2$) channels control neuronal excitability and synaptic plasticity, and have been implicated in substance abuse. However, it is unknown if genes that encode $K_{Ca}2$ channels *(KCNN1-3)* influence alcohol and drug addiction. In the present study, an integrative functional genomics approach shows that genetic datasets for alcohol, nicotine, and illicit drugs contain the family of *KCNN* genes. Alcohol preference and dependence QTLs contain *KCNN2* and *KCNN3*, and *Kcnn3* transcript levels in the nucleus accumbens (NAc) of genetically diverse BXD strains of mice predicted voluntary alcohol consumption. Transcript levels of *Kcnn3* in the NAc negatively correlated with alcohol intake levels in BXD strains, and alcohol dependence enhanced the strength of this association. Microinjections of the $K_{Ca}2$ channel inhibitor apamin into the NAc increased alcohol intake in control C57BL/6J mice, while spontaneous seizures developed in alcohol-dependent mice following apamin injection. Consistent with this finding, alcohol dependence enhanced the intrinsic excitability of medium spiny neurons in the NAc core and reduced the function and protein expression of $K_{Ca}2$ channels in the NAc. Altogether, these data implicate the family of *KCNN* genes in alcohol, nicotine, and drug addiction, and identify *KCNN3* as a mediator of voluntary and excessive alcohol consumption. $K_{Ca}2.3$ channels represent a promising novel target in the pharmacogenetic treatment of alcohol and drug addiction.
Neuropsychopharmacology (2015) **40,** 1928–1939; doi:10.1038/npp.2015.42; published online 4 March 2015

INTRODUCTION

Although the prevalence of alcohol and drug use disorders has increased over the last several decades (Whiteford *et al*, 2013), few efficacious medications are available to treat alcohol and drug addiction. This is likely due to the complex interactions among genetic, epigenetic, and environmental factors that characterize addictive disorders. Based on results from meta-analyses and twin studies, an estimated 23–79% of the variance in alcohol and drug dependence is heritable (Agrawal *et al*, 2012), and matching variations in genes to therapeutics can improve treatment outcomes in individuals with alcohol use disorders (AUDs; Heilig *et al*, 2011; Kranzler and McKay, 2012; Sturgess *et al*, 2011). For example, clinical studies in individuals with AUDs have reported that carriers of the A118G polymorphism in the mu-opiate receptor gene *OPRM1* show a better clinical response to treatment with naltrexone (Anton *et al*, 2008; Anton *et al*, 2012; Oslin *et al*, 2003; Ray and Hutchison, 2007; Schacht *et al*, 2013). Thus, identifying additional genetic factors that contribute to excessive use of alcohol or drugs is critical for developing more efficacious therapies for these disorders.

Small-conductance Ca^{2+}-activated K^+ ($K_{Ca}2$) channels link fluctuations in intracellular Ca^{2+} levels with functional changes in the membrane potential of neurons to regulate neuronal excitability, synaptic plasticity, and learning (Adelman *et al*, 2012). Cloning studies have identified three *KCNN* genes that encode $K_{Ca}2$ channel α subunits in the brain ($K_{Ca}2.1$: *KCNN1* located on human Chr 19 and mouse Chr 8; $K_{Ca}2.2$: *KCNN2*, human Chr 2 and mouse Chr 18; and $K_{Ca}2.3$: *KCNN3*, human Chr 1 and mouse Chr 3; Kohler *et al*, 1996). Although $K_{Ca}2$ channel subunits are widely expressed throughout the brain, their expression pattern varies by brain region (Sailer *et al*, 2002; Sailer *et al*, 2004). $K_{Ca}2.1$ and $K_{Ca}2.2$ channels localize to the cerebral cortex, hippocampus, and lateral amygdala, and $K_{Ca}2.3$ channels are highly expressed in the thalamus, brain stem nuclei, and basal ganglia, including the nucleus accumbens (NAc) and ventral tegmental area (VTA). Although not extensively studied, there is evidence that $K_{Ca}2.2$ and $K_{Ca}2.3$ channel subtypes regulate different aspects of neuronal function. For example, only $K_{Ca}2.2$ channels affect stimulus-evoked excitatory postsynaptic potentials in hippocampal CA1 neurons (Bond *et al*, 2004; Hammond *et al*, 2006; Ngo-Anh *et al*, 2005). $K_{Ca}2.3$ channels influence the frequency of action potential (AP) firing and $K_{Ca}2.2$ and $K_{Ca}2.3$ channels regulate the precision of AP firing in dopamine neurons (Deignan *et al*, 2012; Wolfart *et al*, 2001).

*Correspondence: Dr PJ Mulholland, Department of Neuroscience, Medical University of South Carolina, 67 President Street, IOP 462 North, MSC 861, Charleston, SC 294225-8610, USA, Tel: +1 843 792 1229, Fax: +1 843 792 7353, E-mail: mulholl@musc.edu
Received 28 May 2014; revised 17 January 2015; accepted 26 January 2015; accepted article preview 9 February 2015

In recent preclinical models, modulating $K_{Ca}2$ channel activity regulates alcohol and drug intake. In standard rodent drinking models administration of $K_{Ca}2$ channel-positive modulators reduced operant responding for alcohol and decreased voluntary intake levels (Hopf *et al*, 2010; Hopf *et al*, 2011; Padula *et al*, 2013). Positive modulation of $K_{Ca}2$ channels also attenuated the severity of handling-induced convulsions in alcohol-dependent mice and reduced acute alcohol withdrawal-induced hyperexcitability in cultured hippocampal slices (Mulholland, 2012; Mulholland *et al*, 2011). In addition, chronic alcohol exposure downregulated $K_{Ca}2$ channel function and expression in the hippocampus, NAc, and VTA (Hopf *et al*, 2010; Hopf *et al*, 2007; Mulholland *et al*, 2011). In contrast, repeated cocaine treatment and withdrawal enhanced the $K_{Ca}2$ channel-mediated component of the afterhyperpolarization (AHP) in NAc medium spiny neurons (MSNs; Ishikawa *et al*, 2009; Mu *et al*, 2010). Together, these findings provide compelling evidence that $K_{Ca}2$ channels are involved in alcohol and substance abuse.

To examine the role of the three genes that encode $K_{Ca}2$ channels in regulating alcohol-, nicotine- and illicit drug-related behaviors, the present study employed an integrative functional genomics approach and analyzed databases from clinical and preclinical studies. Results of that analysis demonstrated that the family of *KCNN* genes is present in multiple alcohol- and drug-related quantitative trait loci (QTL) and experimentally derived gene sets. Interestingly, *KCNN2* and *KCNN3* occurred in an alcohol preference QTL on chromosome 18 in genetically diverse BXD recombinant inbred (RI) strains of mice, as well as in an alcoholism susceptibility QTL on human chromosome 1. To better define the role of *KCNN* in voluntary alcohol consumption, we tested a panel of BXD RI strains along with the high-drinking C57BL/6J (B6) and low-drinking DBA/2J (D2) parental strains of mice in two well-established voluntary alcohol consumption models: the drinking in the dark (DID) procedure (Rhodes *et al*, 2005) and an alcohol dependence model of escalated drinking (Becker and Lopez, 2004; Lopez and Becker, 2005). We then used gene and protein expression analysis, electrophysiology, and pharmacological manipulation of $K_{Ca}2$ channel activity to correlate differences in drinking with the functional status of *Kcnn*.

MATERIALS AND METHODS

GeneWeaver Bioinformatics

The GeneWeaver software system (GeneWeaver.org) contains a curated database of functional genomic experimental results across nine species with many types of experimental data including gene expression analyses, QTL positional candidate sets, curated literature annotations for gene functions, chemical interactions, and mutation screens (Baker *et al*, 2012). This database was queried for '*Kcnn1-3* alcohol' and '*Kcnn1-3* drugs' to retrieve clinical and preclinical experiments that implicate these genes in alcohol-, nicotine-, and illicit drug-related experiments. Studies that did not explicitly focus on addiction were excluded. Using a conservative approach, we identified additional genes that were present in at least 70% of the gene sets. Genes were annotated using categories of the Gene Ontology (GO) Consortium (www.geneontology.org), and gene groups were analyzed with a Bonferroni adjusted over-representation test using the PANTHER (Protein ANalysis THrough Evolutionary Relationships) classification system (Mi *et al*, 2013).

Animals and Housing

Male and female C57BL/6J (B6) and DBA/2J (D2) parental strains were purchased from Jackson Laboratory (Bar Harbor, ME), and BXD RI strains were obtained from the University of Tennessee Health Science Center or Jackson Laboratory. Mice were individually housed in temperature- and humidity-controlled environments and kept on a 12-h light/dark cycle. Food and water were available *ad libitum* during all procedures. The Medical University of South Carolina Institutional Animal Care and Use Committee approved all procedures in accordance with NIH guidelines for the humane care and use of laboratory animals.

Chronic Intermittent Ethanol Exposure and Two-Bottle Choice Drinking

To establish baseline drinking, mice consumed alcohol in their home cage using a standard two-bottle choice (15% ethanol (v/v) *vs* water) limited-access (2 h) protocol for 6 weeks. Mice were then underwent four to five repeated weekly cycles of chronic intermittent ethanol (CIE) exposure in vapor inhalation chambers, alternated with weekly home cage drinking sessions (Becker and Lopez, 2004; Griffin *et al*, 2014; Lopez and Becker, 2005). Following the last vapor chamber exposure, mice remained abstinent from alcohol for 72 h prior to sacrifice and tissue collection for microarray analysis. Drinking data were analyzed by two-way ANOVA.

Microarray Data Generation and Analysis

Studies on correlations for *Kcnn1-3* gene expression in NAc were completed using microarray datasets produced from BXD RI strains treated with either saline (Wolen *et al*, 2012) or the CIE protocol (Miles, Smith, Lopez, Becker and Williams, unpublished data). Tissue punch dissections, RNA isolation, and hybridization/scanning procedures with Affymetrix Mouse Genome 430 2.0 arrays (Affymetrix, Cat #900497) were performed as described previously (Wolen *et al*, 2012). Full presentation and discussion of the BXD CIE microarray data will be reported elsewhere (Miles, Smith, Lopez, Becker and Williams, manuscript in preparation). To minimize the risk of technical variation confounding the detection of an alcohol response, we simultaneously processed an air- and CIE-exposed mouse from an individual strain. Annotation data for Mouse Genome 430 2.0 probe sets were obtained from the GeneNetwork Data Sharing Zone (genenetwork.org/share/annotations). Expression data from the air and CIE treatment groups were background corrected, quantile normalized and summarized using the robust multi-array average (RMA) expression measure. All datasets generated for this paper are accessible on GeneNetwork (www.genenetwork.org) and from the Gene Expression Omnibus repository under accession number GSE28515. All data are MIAME compliant.

Phenotype Correlation Analysis

To avoid shared variance across traits inherent to within-subject designs that may artificially inflate correlations, we

analyzed *Kcnn1-3* transcript levels and drinking phenotypes using a between-subjects design across multiple cohorts of experimental mice. First, we conducted a linear regression analysis of *Kcnn1* (probe set 1419617_at), *Kcnn2* (1448927_at), and *Kcnn3* (1421632_at) RMA levels in the NAc of alcohol-naive (saline treated) BXD RI mice from a previous study (Wolen *et al*, 2012) and baseline alcohol intake values from a separate cohort of corresponding BXD RI strains in the CIE-drinking model (as described above). Next, we conducted a linear regression analysis of NAc *Kcnn1-3* RMA levels from air-exposed BXD RI mice and alcohol intake values from the 4-h session on day 4 of a binge alcohol drinking (DID) procedure (Jones, Lu and Williams, unpublished observation, GeneNetwork record ID 13565). Finally, drinking data in air- and CIE-exposed BXD RI mice and their associated NAc *Kcnn3* RMA levels were assessed using a hierarchical linear model (HLM 7.0) with pre-post CIE exposure nested within subject and day further nested within pre-post CIE exposure. Pre-post CIE exposure was fit as a random effect.

Intracranial Stereotaxic Surgery and Microinjections

Adult male B6 mice underwent bilateral cannula placement surgery in the NAc at least 2 weeks prior to the start of the drinking paradigm. Mice received microinjections during the third, fourth, and fifth test drinking sessions as previously described (Griffin *et al*, 2014). Apamin (0–0.8 ng; Sigma-Aldrich, St Louis, MO) was freshly dissolved in sterile saline and was microinfused 30 min prior to the limited access drinking sessions in a dose volume of 0.25 μl/min over 2 min. Cannula placements were verified at the end of the study by cresyl violet staining. Mice were excluded from analysis if the cannula tip was determined to be outside of the NAc as previously described (Griffin *et al*, 2014). Drinking data in mice that received microinjections were analyzed by two-way ANOVA.

Electrophysiology Recordings

We used standard whole-cell patch-clamp electrophysiology procedures and measured intrinsic excitability, AHP amplitude, and $K_{Ca}2$-mediated tail currents in MSNs from adult C57BL/6J mice. Acute slices (300 μm thick) were prepared from C57BL/6J mice following 3–7 days withdrawal from four cycles of CIE exposure to match the time point of the apamin microinjection study. In this cohort of CIE-exposed mice used for recordings, the BEC was 206.8 ± 11.03 mg/dl ($n = 8$ per mice group). Mice were decapitated and the brain was immediately removed and placed in an ice-cold dissection solution consisting of (in mM): 200 sucrose, 1.9 KCl, 1.2 NaH_2PO_4, 6.0 $MgCl_2$, 0.5 $CaCl_2$, 0.4 ascorbate, 10 glucose, and 25 $NaHCO_3$. Slices were incubated at 34°C for 30 min and then kept at room temperature for at least 30 min in artificial cerebral spinal fluid (ACSF) solution containing (in mM): 125 NaCl, 2.5 KCl, 1.25 NaH_2PO_4, 1.3 $MgCl_2$, 2.0 $CaCl_2$, 0.4 ascorbate, 10 glucose, and 25 $NaHCO_3$. After incubation, slices were transferred to a submerged recording chamber bathed in 34°C ACSF. Incubation and recording buffers were continuously aerated with 5% carbon dioxide/95% oxygen. The pH of all solutions listed above was adjusted to 7.3 using NaOH, and osmolarity was measured to be ~300 mOsm. Recordings were made with a Multiclamp 700B amplifier (Axon Instruments, Union City, California) connected to a computer running Windows XP and Axograph X software. Patch pipettes (2–3 MΩ resistance) were pulled from thin-wall borosilicate glass (1.17 mm ID; Warner Instruments, Hamden, CT, USA) and filled with internal solution (pH 7.3 using KOH, osmolarity ~290 mOsm) containing (in mM): 140 K-methylsulfate, 8.0 NaCl, 1.0 $MgCl_2$, 0.05 EGTA, 10 HEPES, and 5 Mg_2 ATP. Currents were acquired at 10 kHz using an ITC-18 interface. To activate $K_{Ca}2$-mediated tail currents, neurons were held at −70 mV and depolarizing voltage steps (400 ms, from −30 to +10 mV in 10 mV increments) were applied with 2 s between each step. The protocol was repeated three times followed by a 10-min bath application of 100-nM apamin and three additional recordings. The data were averaged for each of the three protocols, and peak amplitude of the $K_{Ca}2$-mediated tail current that occurred up to 100 ms after each depolarizing pulse was measured. To determine the effects of withdrawal from CIE on AP spiking of neurons in the NAc core, current-clamp recordings were performed. Spike firing was induced by direct current injection (from 0 to 220 pA with 20 pA increments) through patch pipettes filled with K-methylsulfate internal solution (recipe as described above). Recordings were analyzed for number of spikes in response to each injected current, resting membrane potential (mV), frequency (Hz), interspike interval (ISI, msec), and AHP (mV). The first three AHP magnitudes were averaged, in which each AHP magnitude was calculated by subtracting the lowest potential during hyperpolarization from AP threshold. Averaged peak amplitude of the $K_{Ca}2$-mediated tail currents at each step before and after application of apamin was analyzed by two-way ANOVA. Differences in AP and AHP parameters between air-treated and CIE groups were analyzed by two-way ANOVA or unpaired two-tailed *t*-test.

Western Blotting

Tissue punches targeting the NAc core were extracted from a separate cohort of male B6 mice immediately following completion of their last drinking test session, flash frozen and stored at −80°C until processing. Samples were solubilized in 2% LDS and western blotting was performed using a primary antibody directed against $K_{Ca}2.3$ channels (1 : 4000; Alomone Labs, Jerusalem, Israel). An aliquot of each sample was taken for determination of protein concentration by the bicinchoninic acid assay (Pierce Biotechnology, Rockford, IL). Samples were diluted with NuPAGE 4X LDS sample loading buffer (Invitrogen Corp., Carlsbad, CA; pH 8.5) containing 50-mM dithiothreitol, and denatured for 10 min at 95°C. Approximately, 5 μg of each sample was separated using the Bis-Tris (375 mM resolving buffer and 125-mM stacking buffer, pH 6.4; 7.5% acrylamide) discontinuous buffer system with MOPS electrophoresis buffer (50-mM MOPS, 50-mM Tris, 0.1% SDS, and 1-mM EDTA, pH 7.7). Protein was then transferred to Immobilon P PVDF membranes (Millipore, Bedford, MA) using a semi-dry transfer apparatus (Bio-Rad Laboratories, Hercules, CA). After transfer, blots were washed with phosphate-buffered saline containing 0.1% Tween 20 (PBST) and then blocked with PBST containing 5% nonfat dried milk (NFDM) for 1 h at room temperature with agitation. The membranes were then

Table 1 Gene Sets from GeneWeaver Related to Alcohol-, Nicotine-, and Illicit Drug-Related Behaviors that Contain the Family of *KCNN* Genes

Gene	Drug	Gene Set	Description	Number of Genes	Pubmed ID
KCNN1	Alcohol	GS84205	Chronic alcohol withdrawal severity (Published QTL, Chr 8)	421	12925894
	Alcohol	GS128597	Ethanol Induced Ataxia, Chr 8	704	N/A
	Alcohol	GS128577	Ethanol induced LORR, Chr 8	836	N/A
	Cocaine	GS84204	Differences in cocaine responsiveness (Published QTL, Chr 8)	345	7932176
	Meth	GS84206	Methamphetamine responses for body temperature (Published QTL, Chr 8)	573	8987796
	Morphine	GS35699	Neocortex Gene expression correlates of Morphine distance (cm) travelled minutes 105–120 in Females BXD	20	19958391
	Morphine	GS36357	Whole Brain Gene expression correlates of Naloxone induced Morphine Withdrawal - TOTAL vertical activity counts in 15 min in Males BXD	22	19958391
	Morphine	GS33943	Neocortex Gene expression correlates of Morphine distance (cm) travelled minutes 120–135 in Females & Males BXD	61	19958391
	Morphine	GS87119/ GS87379	Transcriptional profiling of C57 and DBA strains of mice in the absence and presence of morphine	178	17367521
KCNN2	Alcohol	GS746	EtOH preference in female BXD RI strains	96	7695038
	Alcohol	GS137407	Network analysis of gene expression in three brain regions of human alcoholics and control cases identifies distinct modules of co-expressed genes	3178	22302827
	Alcohol	GS128199	Alcohol Preference union of 86 Gene Sets	8392	N/A
	Morphine	GS86906/ GS87380	Morphine effects on striatal transcriptome in mice. Analyze the effects of single and repeated morphine administrations in selected inbred mouse strains	2537/2693	17598886
	Nicotine	GS123199	Tobacco Smoke Pollution interacting genes incorporated from 24 publications in the Comparative Toxicogenomics Database	201	N/A
KCNN3	Alcohol	GS128625	Alcohol response QTL 17 (Alcrsp17 Published QTL, Chr 2)	956	16953387
	Alcohol	GS84150	Ethanol conditioned taste aversion (Published QTL, Chr 3)	631	9756038
	Alcohol	GS128572	Ethanol Induced Hypothermia, Chr 3	844	N/A
	Alcohol	GS218390	Alcoholism susceptibility, Chr 1	2187	15211641
	Cocaine	GS35833	Hippocampus Gene expression correlates of Cocaine CPP	37	19958391
	Heroin	GS86977	Distinctive Profiles of Gene Expression in the Human Nucleus Accumbens Associated with Heroin Abuse	911	16710320
	Meth	GS84151	Methamphetamine responses for body temperature (Published QTL, Chr 3)	631	8987796
	Poly-Drug	GS136769	Suppressor of superoxide production (Susp, Published QTL, Chr 3)	344	11937300
	Nicotine	GS14888	Differentially expressed genes modulated by nicotine in five combined brain regions (Amyg, HP, NA, PFC and VTA) for C3H/He mice	263	17504244
	Nicotine	GS14904	Genes harboring allelic variants that distinguish successful *vs* unsuccessful nicotine Abstainers	107	18519826

incubated overnight at 4°C with the primary antibody diluted in PBST containing 0.5% NFDM and washed in PBST prior to 1-h incubation at room temperature with horseradish peroxidase-conjugated secondary antibodies diluted 1 : 2000 in PBST. Membranes received a final wash in PBST and the antigen-antibody complex was detected by enhanced chemiluminescence using a ChemiDoc MP Imaging system (Bio-Rad Laboratories, Hercules, CA). Bands were quantified by mean optical density using computer-assisted densitometry with ImageJ v1.41 (National Institutes of Health, USA). Because controls (eg, actin and GAPDH) used to normalize protein loading in western blot experiments can actually cause quantitation errors (Aldridge *et al*, 2008; Dittmer and Dittmer, 2006; Welinder and Ekblad, 2011), we used methods described by Aldridge *et al*, 2008 for normalizing to a total protein stain (Swift membrane stain; G Biosciences, St Louis, MO). Normalized protein expression data were analyzed with a two-tailed *t*-test. Analysis of the optical density values for the total protein stain demonstrated that the amount of protein loaded did not differ between the samples from the air and CIE-exposed mice ($t(11) = 0.203$; $p = 0.843$; $n = 6–7$ per group).

RESULTS

KCNN1-3 and Alcohol, Nicotine, and Drug Addiction

The plausibility of a role for the family of *KCNN* genes in the behavioral effects of alcohol and other drugs of abuse was evaluated by the GeneWeaver database search of previous whole genome studies in which *KCNN1-3* has been associated with alcohol- and drug-related behaviors. As shown in Table 1, multiple alcohol- and drug-related QTLs and gene sets from human and rodent studies contain *KCNN1-3* genes. Moreover, this search showed that exposure to alcohol, opiates, or nicotine also significantly altered expression of *KCNN1-3* in the NAc, superior frontal gyrus, or basolateral amygdala (Supplementary Table 1). Findings from this integrative

genomics approach provide strong evidence that the family of *KCNN* genes are involved in alcohol, nicotine and illicit drug addiction and dependence and are consistent with evidence suggesting genetic overlap in substance use disorders (Agrawal *et al*, 2012). Although we identified *KCNN1* and *KCNN2* in some gene sets related to drugs of abuse, only *KCNN3* is contained in gene sets for all of the drugs of abuse. Thus, we next asked whether other genes in these QTLs and gene sets were highly related to alcohol and drug addiction. As shown in Table 2 and Supplementary Figure 1, 70% or more of these gene sets also contain eight other genes (*S100A6*, *S100A8*, *S100A9*, *SYT11*, *SHC1*, *JTB*, *GATAD2B*, and *RAB13*). To identify whether specific signaling pathways were present in this network, we analyzed these genes with an over-representation test using PANTHER software (Mi *et al*, 2013). There were two PANTHER protein classes (intracellular Ca^{2+}-sensing proteins and calmodulin) and one GO molecular function category (calmodulin binding) that were significantly over-represented (Bonferroni-adjusted over-representation test; $p<0.05$) in this gene network. These results support the idea that genes related to intracellular Ca^{2+} signaling and $K_{Ca}2$ channel function are positional candidates that may contribute to substance abuse.

Kcnn3 Levels in the NAc Predict Drinking in Mice

Because *KCNN2* occurred in an alcohol preference QTL on chromosome 18 in female BXD mice and *KCNN3* occurred in an alcoholism susceptibility locus on human chromosome 1, we explored the relationship between *KCNN* genes and alcohol intake. First, we correlated NAc *Kcnn1-3* RMA values obtained from alcohol-naive mice (Wolen *et al*, 2012) with baseline drinking data obtained from corresponding BXD RI strains of mice in the present study ($n=14$ strains; 106 total mice). Transcript levels of each *KCNN* gene in the NAc varied across the BXD strains (*Kcnn1*: 7.58 ± 0.114 (mean transcript expression levels ± SD), 1.53-fold range; *Kcnn2*: 9.59 ± 0.099, 1.30-fold range; *Kcnn3*: 7.46 ± 0.112, 1.44-fold range; Figure 1a). Similarly, average daily voluntary alcohol consumption by BXD mice during the 6-week baseline period varied across strains (Figure 1b). Linear regression analyses demonstrated that *Kcnn3*, but not *Kcnn1* or *Kcnn2* RMA values, significantly predicted average daily baseline drinking levels in these mice (*Kcnn1*: $R^2=0.033$, $p=0.54$; *Kcnn2*: $R^2=0.024$, $p=0.57$; *Kcnn3*: $R^2=0.373$, $p<0.05$; Figure 1c) with high transcript levels of *Kcnn3* in the NAc of BXD strains associated with low intake of alcohol. To further explore the negative relationship between *Kcnn3* transcript levels and alcohol drinking, we analyzed *Kcnn1-3* RMA values in air-exposed mice and drinking levels of BXD strains from the DID procedure (GeneNetwork record ID 13565; Supplementary Figure 2a). As shown in Supplementary Figure 2b, alcohol intake during the 4-h drinking session varied across BXD strains on day 4 of the DID procedure. Similar to results in the two-bottle choice limited-access model, RMA values for *Kcnn3*, but not *Kcnn1* or *Kcnn2*, significantly predicted binge-like drinking in the DID model (Supplementary Figure 2c). In both the two-bottle choice and DID limited access models, *Kcnn3* RMA values in the NAc were negatively associated with alcohol intake in BXD mice.

Next, we used a HLM to analyze the relationship between *Kcnn3* RMA values and alcohol consumption in BXD mice exposed to the CIE treatment. We selected HLM regression for this analysis because the predictor variables of the CIE dependence model vary at more than one level, and HLM can account for the shared variance in hierarchical data (Woltman *et al*, 2012). As shown in Figure 2a, a significant negative relationship occurred between *Kcnn3* RMA values in the NAc and the amount of alcohol consumed during the 6-week baseline period of the study (air controls: $b=-1.99$, SE = 0.76, $t(52)=2.61$, $p=0.012$; CIE mice: $b=-2.61$, SE = 0.96, $t(52)=2.72$, $p=0.009$; $n=28$ strains, 114 total mice). These results are consistent with those depicted in Figure 1c and Supplementary Figure 2c, and suggest that *Kcnn3* expression in the NAc predicts drinking among non-dependent BXD strains. In addition, the relationship between amount consumed and *Kcnn3* RMA values in the NAc of dependent mice was even more robust (*Kcnn3* slope *x* treatment interaction: $b=-1.12$, SE = 0.55, $t(51)=2.04$, $p<0.05$). That is, the *Kcnn3* slope was more extreme and declined more rapidly with increasing *Kcnn3* RMA levels in CIE-exposed BXD mice compared to air-exposed controls (Figure 2b). Although only a modest effect, intercept values (drinking extrapolated to 0 *Kcnn3*) were significantly higher in CIE-exposed BXD mice than controls (intercept values: $b=7.63$, SE = 3.79, $t(51)=2.01$, $p<0.05$).

Blocking $K_{Ca}2$ Channels in the NAc Modulates Drinking in B6 Mice

The relationship between *Kcnn3* expression levels in the NAc during baseline drinking and following CIE exposure suggests that $K_{Ca}2.3$ channels in the NAc may regulate consumption and escalation of drinking in CIE-exposed mice. To further test this hypothesis, we bilaterally microinjected the potent and selective $K_{Ca}2$ channel allosteric inhibitor apamin into the NAc of air control and CIE-exposed B6 mice. Microinfusions began during the third drinking test cycle and continued through the fourth and fifth test cycles when higher drinking levels are typically observed in CIE-exposed mice (Griffin *et al*, 2014; Griffin *et al*, 2009). We microinjected vehicle (0.9% sterile saline) or apamin (0.2–0.8 ng/0.5 μl) 30 min prior to each drinking session in a quasi-random manner. As expected, CIE-exposed mice microinfused with vehicle consumed significantly more alcohol than air-exposed mice (two-way ANOVA, group *x* dose interaction, $F(3,126)=4.481$, $p=0.005$, SNK *post-hoc*, $p<0.05$, $p<0.001$, $n=8$–32 per group; Figure 3a). Microinfusion of a 0.4-ng dose of apamin significantly increased consumption in air-exposed mice, but not in dependent mice (Figure 3a). Although the high dose of apamin (0.8 ng) did not affect drinking in controls, it unexpectedly decreased voluntary consumption in CIE-exposed mice (Figure 3a). Histological confirmation of cannula placement is shown in Figure 3b and c. Monitoring behavior during and after the drinking sessions revealed an enhanced behavioral sensitivity to apamin in CIE-exposed mice that may have affected drinking. Thus, while only one of nine air-control mice displayed mild behavioral impairment (ie, involuntary twitching) after drug administration, 50% of the CIE-exposed mice developed spontaneous tonic/clonic seizures following the high-dose apamin infusion (χ^2 for trend $(1, n=15)=4.650$, $p<0.05$; Figure 3d).

Table 2 A Conservative Network of Genes Found Within 70% or more of Alcohol-, Nicotine-, and Illicit Drug-Related GeneWeaver Gene Sets that also Contain *KCNN3*

Gene name	Protein name	PANTHER protein class	GO molecular function	GO biological process	GO cellular component
GATAD2B	Transcriptional repressor p66-β	Chromatin/chromatin-binding protein	Nucleic acid binding; chromatin binding	Sequence-specific DNA-binding transcription factor activity; regulation of transcription from RNA polymerase II promoter; chromatin organization	Nuclear speck
JTB	Protein JTB	N/A	Protein kinase binding	Apoptotic mitochondrial changes; positive regulation of protein kinase activity; cytokinesis	Centrosome; mitochondrion
KCNN3	K_{Ca}2.3 channel	Small conductance calcium-activated K+ channel activity	Cation channel activity; calmodulin binding	Potassium ion transmembrane transport; synaptic transmission	Plasma membrane
RAB13	Ras-related protein Rab-13	N/A	GTP binding; GTPase activity	Actin cytoskeleton organization; establishment of protein localization to plasma membrane; endocytic recycling	Cytoplasmic vesicle membrane; recycling endosome; trans-Golgi network
S100A6	Protein S100-A6	Growth factor; calmodulin	Calcium ion binding; growth factor activity; calmodulin binding	Macrophage activation; DNA replication; cell cycle; cell communication	Cytosol; extrinsic component of cytoplasmic side of plasma membrane
S100A8	Protein S100-A8	Growth factor; calmodulin	Calcium ion binding;Toll-like receptor 4 activity; calmodulin binding	Macrophage activation; DNA replication; cell cycle; cell communication	Cytosol; extracellular vesicular exosome
S100A9	Protein S100-A9	Signaling molecule; calmodulin	Calcium ion binding; calmodulin binding; receptor binding	Autophagy; DNA replication; cell-cell signaling; chronic inflammation response	Cytosol; extracellular vesicular exosome; nucleus
SHC1	SHC-transforming protein 1	Signaling molecule	Epidermal growth factor receptor binding; protein tyrosine kinase activity	Ras protein signal transduction; positive regulation of DNA replication and cell proliferation; nervous system development	Cytosol; mitochondrial matrix
SYT11	Synaptotagmin-11	Membrane trafficking regulatory protein	Transporter activity	Synaptic transmission; neurotransmitter secretion; intracellular protein transport; synaptic vesicle exocytosis	Synaptic vesicle membrane

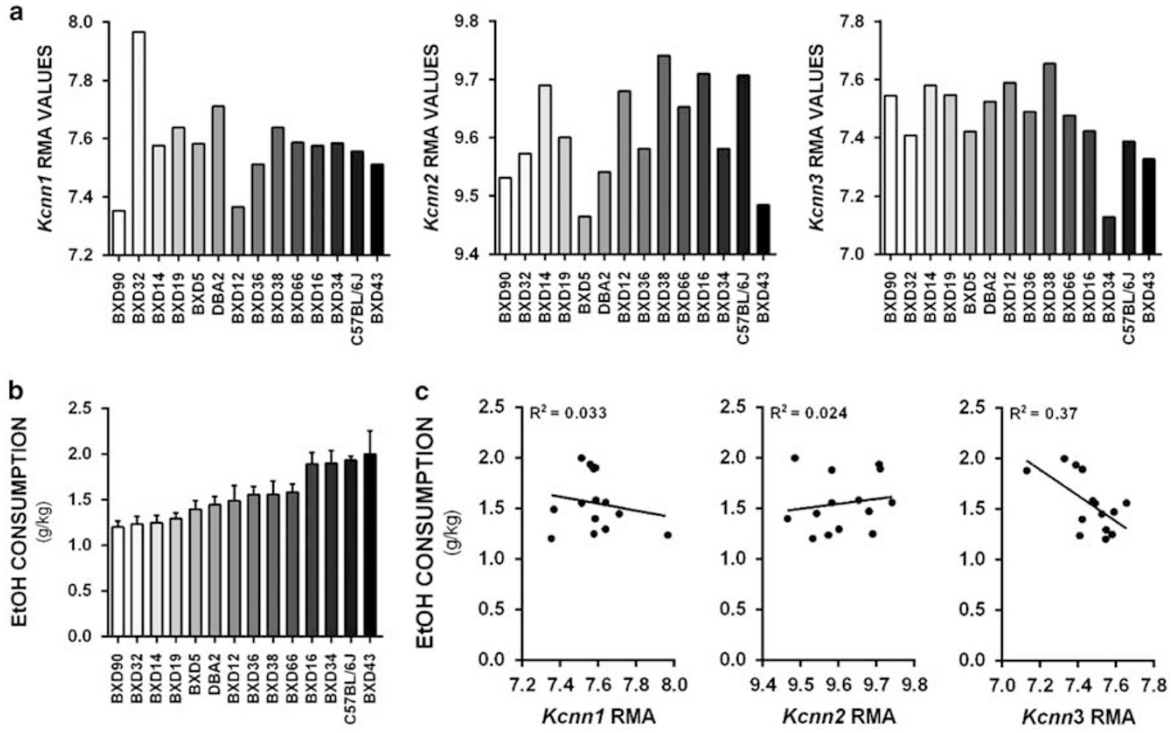

Figure 1 *Kcnn3* RMA values in the NAc of saline-treated BXD RI mice predict average daily voluntary alcohol (15% v/v) consumption in BXD RI strains of mice. (a) *Kcnn1-3* RMA values in the NAc of alcohol-naive saline-treated BXD RI mice. (b) Average alcohol consumption levels during the 6-week baseline period in air-exposed BXD strains in the two-bottle choice limited access model ($n = 14$ strains, 106 total mice). (c) Regression analysis of *Kcnn1-3* RMA values in the NAc of saline-treated mice and average baseline alcohol intake levels in non-dependent BXD RI strains of mice (*Kcnn1*: $R^2 = 0.033$, $p = 0.54$; *Kcnn2*: $R^2 = 0.024$, $p = 0.57$; *Kcnn3*: $R^2 = 0.373$, $^*p < 0.05$).

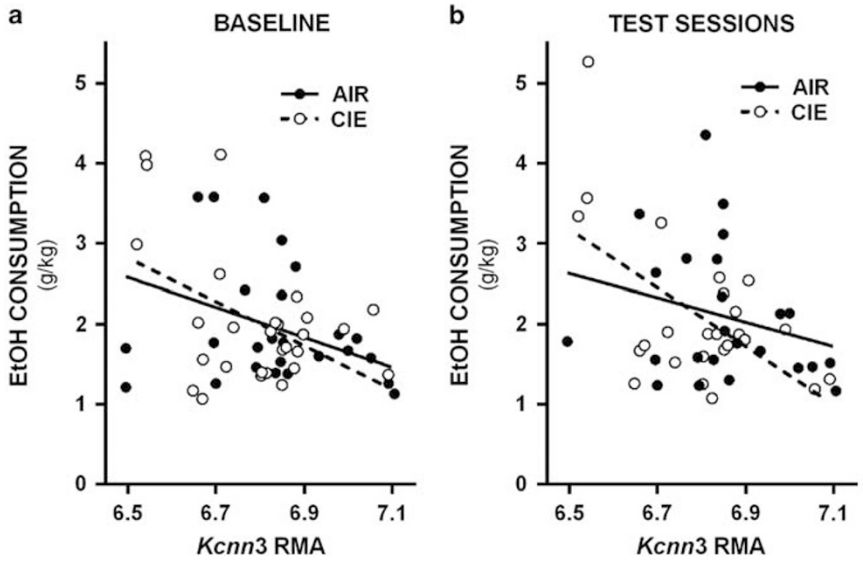

Figure 2 *Kcnn3* transcript levels in the NAc predict baseline and CIE-induced escalation of drinking in BXD RI strains of mice. (a) A negative relationship occurred between *Kcnn3* RMA values in the NAc and average alcohol consumption levels during the 6-week baseline period in air- and CIE-exposed BXD strains (air controls: $b = -1.99$, SE = 0.76, $t(52) = 2.61$, $^*p = 0.012$; CIE mice: $b = -2.61$, SE = 0.96, $t(52) = 2.72$, $^*p = 0.009$; $n = 28$ strains, 114 total mice). (b) Graph of NAc *Kcnn3* RMA levels in air- and CIE-exposed mice in relation to average alcohol drinking during the test drinking sessions (*Kcnn3* slope (ie, slope by treatment interaction): $b = -1.12$, SE = 0.55, $t(51) = 2.04$, $^*p < 0.05$; intercept values: $b = 7.63$, SE = 3.79, $t(51) = 2.01$, $^*p < 0.05$).

CIE-Induced Functional Adaptations in Intrinsic Excitability and $K_{Ca}2$ Channels in the NAc

To determine if hypersensitivity of CIE mice to apamin was due to functional adaptations, we first examined CIE-induced changes in intrinsic excitability of MSNs in the NAc core using whole-cell slice electrophysiology. We performed the recordings at the same time point as the drinking studies to parallel the apamin microinjection experiment described above. CIE exposure did not alter the

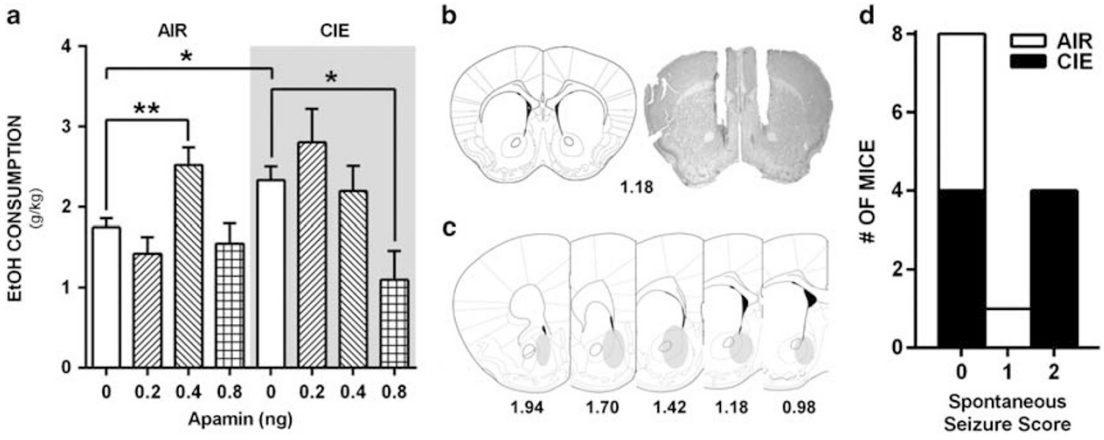

Figure 3 Pharmacological inhibition of $K_{Ca}2$ channels in the NAc modulates alcohol drinking and behavior differently in air- and CIE-exposed B6 mice. (a) Apamin (0–0.8 ng in 0.5 μl) was microinjected into the NAc of air controls and CIE-exposed mice (two-way ANOVA, group *x* dose interaction, $F(3,126) = 4.481$, $p = 0.005$, SNK *post hoc*, $^*p < 0.05$, $^{**}p < 0.001$, $n = 8$–32 per group). (b) Representative cresyl violet stained tissue sections showing typical placements for the bilateral microinjector guides and tips. (c) A schematic of the plates from the Paxinos (2007) atlas demonstrates the locations of the tips of the microinjection cannula targeting the NAc. (d) Microinjection of 0.8 ng of apamin into the NAc of dependent C57BL/6J mice significantly increased the occurrence of seizure-like activity (0 = normal behavior, 1 = myoclonic jerks, 2 = spontaneous tonic/clonic seizures; χ^2 for trend ($1, n = 15$) = 4.650, $^*p < 0.05$).

resting membrane potential (air: -69.6 ± 1.36 mV, CIE: -70.85 ± 1.37; *t*-test, $t(18) = 0.697$, $p = 0.49$, $n = 8$–12 per group), but significantly increased basal firing rates of MSNs in the NAc core (two-way ANOVA, $F(1,162) = 35.34$, $p < 0.0001$; Figure 4a). CIE exposure also markedly enhanced AP frequency (*t*-test, $t(18) = 3.395$, $p = 0.003$, $n = 8$–12 per group; Figure 4b) and decreased AP ISI (*t*-test, $t(18) = 3.618$, $p = 0.002$, $n = 8$–12 per group; Figure 4c). Since $K_{Ca}2$ channels regulate intrinsic excitability by enhancing the AHP of NAc core neurons (Hopf *et al*, 2010), we examined the effects of CIE exposure on the AHP amplitude. CIE mice showed a significant reduction in AHP amplitude (*t*-test, $t(18) = 3.078$, $p = 0.007$, $n = 8$–12 per group; Figure 4d), providing additional evidence that CIE exposure decreases $K_{Ca}2$ channel function.

We then applied depolarizing voltage steps in MSNs to activate $K_{Ca}2$ channel outward tail currents. As shown in Figure 4e–g, bath application of 100 nM apamin blocked the peak tail current in air-exposed mice (two-way ANOVA, $F(1,65) = 9.671$, $p = 0.002$, $n = 11$ neurons). CIE exposure significantly reduced the peak tail current in comparison with currents recorded from controls (two-way ANOVA, $F(1, 24) = 7.925$, $p = 0.009$, $n = 11$–15 neurons; Figure 4f and h), without altering cell capacitance values (two-tailed *t*-test, $t(24) = 1.55$, $p = 0.134$, data not shown). Bath application of apamin did not affect the peak tail currents in MSNs recorded from dependent mice, in contrast with control mice (two-way ANOVA, $F(1, 115) = 0.1883$, $p = 0.67$, $n = 15$ neurons; Figure 4f and i). Altogether, these data suggest that CIE exposure produces profound adaptations in $K_{Ca}2$-mediated processes likely caused by a downregulation of functional $K_{Ca}2.3$ channels expressed in MSNs in the NAc core.

In a separate cohort of B6 mice ($n = 17$–19/group), baseline alcohol consumption was established and then the mice were treated with repeated weekly cycles of CIE exposure alternated with test drinking sessions. As shown in Figure 5a, CIE exposure significantly increased drinking in comparison with air-exposed controls during test cycles 1 and 3 (two-way ANOVA, group *x* test session interaction, $F(4,136) = 3.190$, $p = 0.015$, SNK *post-hoc*, $p < 0.05$ *vs* air). We extracted tissue punches targeting the NAc core from these air- and CIE-exposed mice after their last drinking session and used western blotting to examine protein expression. Consistent with the electrophysiology results, CIE exposure significantly reduced $K_{Ca}2.3$ channel protein levels in the NAc core ($t(11) = 2.511$, $p < 0.05$, $n = 6$–7 per group; Figure 5b and c).

DISCUSSION

A major finding of this study is that *KCNN* genes exist in multiple alcohol- and drug-related QTLs and gene sets from both clinical and preclinical studies. Moreover, alcohol, opiates, and nicotine alter expression of *KCNN* genes in critical brain regions, further implicating these genes in substance abuse. Our study also showed that *KCNN3* is in a gene set for an alcoholism susceptibility locus located on human chromosome 1. In support of this clinical observation, *Kcnn3* transcript levels in the NAc of genetically diverse BXD strains predicted baseline alcohol intake in two limited-access drinking models (two-bottle choice and DID). Alcohol-dependent mice with low *Kcnn3* RMA levels consumed more alcohol than controls with equivalent *Kcnn3*, and higher *Kcnn3* levels protected against CIE-induced escalation of drinking in alcohol-dependent mice. These findings suggest that low *KCNN3* expression and function may be a risk factor for developing AUD.

Previous studies reported that chronic alcohol exposure reduced the function and expression of $K_{Ca}2$ channels in the NAc, VTA, and hippocampus of rodents (Hopf *et al*, 2010; Hopf *et al*, 2007; Mulholland *et al*, 2011). Extending these preclinical findings, the integrative functional genomic analysis identified a gene set showing a decrease of *KCNN2* in the superior frontal gyrus and the basolateral amygdala of alcoholics (Ponomarev *et al*, 2012). Notably, in opposition to the effect of chronic alcohol exposure on $K_{Ca}2$ channels, we found that psychostimulants and heroin increased *KCNN3* expression or function of $K_{Ca}2$ channels in the NAc

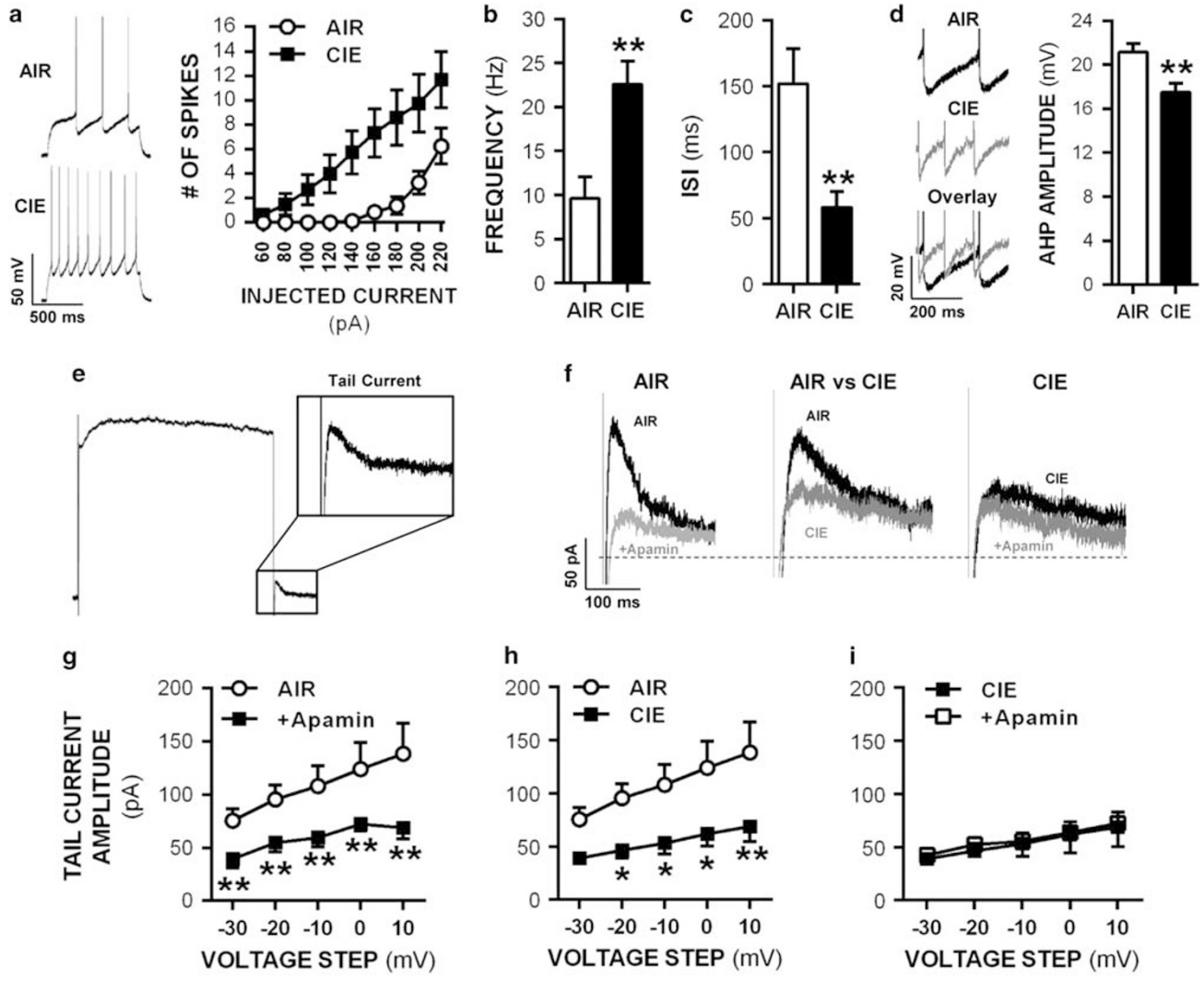

Figure 4 CIE exposure enhances intrinsic excitability and reduces the amplitude of the afterhyperpolarization (AHP) and $K_{Ca}2$ channel-mediated tail currents in MSNs in the NAc core. (a) Representative traces and quantitation show enhanced current-evoked AP firing in CIE-exposed mice (*$p<0.05$; $n=8$–12 neurons per group). (b, c) CIE exposure significantly alters the frequency and the interspike interval of MSNs. (d) CIE exposure reduces AHP amplitude (**$p<0.01$; $n=8$–12 neurons per group). (e) Representative trace showing a voltage step from −70 to +10 mV and the apamin-sensitive tail current that occurs after returning to −70 mV. (f) Examples of traces from tail currents recorded from NAc core MSNs in air- and CIE-exposed mice. Also shown are traces demonstrating the ability of 10 min bath application of 100 nM apamin to block these tail currents in air-exposed mice. (g–i) Quantitation of $K_{Ca}2$ channel-mediated tail currents in air- and CIE-treated mice before and after bath application of apamin (*$p<0.05$, **$p<0.01$; $n=11$–15 neurons per group).

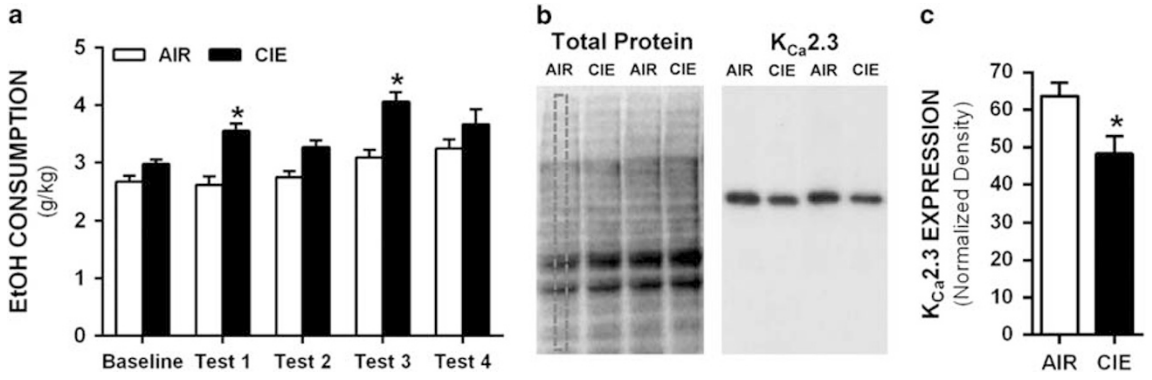

Figure 5 Dependence-induced escalation of drinking reduces $K_{Ca}2.3$ channel expression in the NAc core. (a) CIE-induced escalation of alcohol drinking in dependent B6 mice (two-way ANOVA, group *x* test session interaction, $F(4,136)=3.190$, $p=0.015$, SNK *post hoc*, *$p<0.05$ *vs* air). (b) Representative images of the total protein stain (5 μg per lane) and blot of $K_{Ca}2.3$ channels in air- and CIE-exposed B6 mice. The dashed box in lane 1 represents the quantified area of the total protein stain. (c) Normalized protein expression levels of $K_{Ca}2.3$ channels in air- and CIE-exposed B6 mice that have been drinking alcohol in the CIE-induced escalation of drinking model (two-tailed *t*-test, $t(11)=2.511$, *$p<0.05$, $n=6$–7 per group).

(Albertson *et al*, 2006; Ishikawa *et al*, 2009; Mu *et al*, 2010; Wang *et al*, 2008; Supplementary Table 2). Chronic morphine treatment also altered *KCNN1* transcript levels in the mouse NAc (Grice *et al*, 2007), although the authors did not report the direction of the change. The findings of the present study add to a growing literature showing that alcohol, nicotine, and illicit drugs significantly alter $K_{Ca}2$ channel expression and function in key regions within the addiction neurocircuitry.

Congruent with our findings that low *Kcnn3* transcript levels in the NAc are associated with higher alcohol intake, we demonstrated that pharmacological inhibition of $K_{Ca}2$ channels in the NAc increased alcohol consumption in B6 mice. Previous evidence has demonstrated that positive modulators of the $K_{Ca}2$ channel decrease operant responding for alcohol and voluntary drinking in non-dependent rats and mice (Hopf *et al*, 2010; Hopf *et al*, 2011; Padula *et al*, 2013). Our data show that apamin can increase drinking, provide strong evidence that $K_{Ca}2$ channels in the NAc bi-directionally modulate alcohol intake. In addition to demonstrating the genetic relationship between *Kcnn3* and alcohol intake in mice, the results of the present study also show that CIE exposure produces neuroadaptations in accumbal $K_{Ca}2$ channels. Microinfusions of a higher dose of apamin into the NAc produced spontaneous seizures only in dependent mice and this heightened susceptibility was associated with enhanced intrinsic excitability of NAc MSNs, a reduction in the amplitude of their AHP and $K_{Ca}2$-mediated tail currents and downregulation of $K_{Ca}2.3$ channel protein levels. These findings are consistent with the known role for the $K_{Ca}2.3$ channel as a low-pass filter that regulates firing frequency (Deignan *et al*, 2012; Wolfart *et al*, 2001). Since blocking $K_{Ca}2$ channels in control B6 mice increases drinking to levels comparable to those observed in dependent mice, we speculate that the neuroadaptations in $K_{Ca}2.3$ channels produced by CIE exposure may contribute to escalation of drinking associated with dependence.

Evidence suggests a genetic overlap in individuals addicted to alcohol, nicotine, or illicit drugs (Agrawal *et al*, 2012), and our functional genomic analysis implicates *KCNN1-3* in QTLs and behaviors directly related to alcohol and drug intake. Along with *KCNN3*, results from our bioinformatic analysis in alcohol- and drug-related QTLs and gene sets identified a conservative subset of genes related to intracellular calcium signaling and calmodulin binding. These data suggest that these gene networks may contribute to individual differences in vulnerability to alcohol and drug abuse and dependence. Importantly, there is a genetic basis underlying the ability to remain abstinent during withdrawal from harmful drug intake (Crettol *et al*, 2006; Crettol *et al*, 2005; Fonseca *et al*, 2011; Uhl *et al*, 2008), and findings from genomic studies support the use of personalized medicines for treating addictions (Deschaux *et al*, 1997; Heilig *et al*, 2011; Kranzler and McKay, 2012; Sturgess *et al*, 2011). Indeed, matching SNPs in the *OPRM1* gene to naltrexone treatment leads to more successful clinical outcomes in individuals with AUDs (Anton *et al*, 2008; Anton *et al*, 2012; Oslin *et al*, 2003; Ray and Hutchison, 2007; Schacht *et al*, 2013). In addition, polymorphisms in genes that encode methadone-metabolizing enzymes and transporter proteins contribute to low methadone plasma concentrations and ineffective methadone maintenance treatment programs (Crettol *et al*, 2006; Crettol *et al*, 2005; Fonseca *et al*, 2011). Studies also provide evidence that variants related to dopamine transmission can predict successful smoking cessation (Johnstone *et al*, 2004; Lerman *et al*, 2006; Swan *et al*, 2005; Uhl *et al*, 2008). Interestingly, *KCNN3* is found in convergent genome-wide association studies of successful smoking abstainers (Uhl *et al*, 2008), and $K_{Ca}2$ channels can modulate evoked DA release and dopaminergic neurotransmission (Deignan *et al*, 2012; Herrik *et al*, 2012; Jacobsen *et al*, 2008; Soden *et al*, 2013). A number of polymorphisms in *KCNN3* have been reported (Bowen *et al*, 2001; Chandy *et al*, 1998; Grube *et al*, 2011), and these polymorphisms reduce surface trafficking and currents from $K_{Ca}2$ channels (Chandy *et al*, 1998; Grube *et al*, 2011; Miller *et al*, 2001; Soden *et al*, 2013). However, whether individuals with *KCNN3* polymorphisms that reduce $K_{Ca}2$ channel function have a higher risk for developing an AUD is still unknown. Thus, it will be important to determine whether $K_{Ca}2$ channel ligands are a suitable treatment for alcohol, nicotine, and illicit drug abuse, and whether *KCNN* polymorphisms predict effective treatment outcomes in substance abusers.

In the present study, blocking $K_{Ca}2$ channels in the NAc increased drinking presumably by enhancing neuronal activity of MSNs. MSNs in the dorsal and ventral striatum segregate into two distinct populations that are intermixed and indistinguishable in morphology. However, MSN subtypes express different genes, project to distinct brain regions, and have opposing roles in motivated and goal-directed behaviors (Heiman *et al*, 2008; Keeler *et al*, 2014). D1-dopamine receptor (D1DR)-expressing MSNs in the direct pathway project to the ventral pallidum, globus pallidus interna, substantia nigra pars reticulata, and VTA, while D2DR-expressing MSNs in the indirect pathway project to the globus pallidus externa. Although these pathways work together to balance ongoing normal behavior, mounting evidence suggests that drugs of abuse and chronic stress alters the balance between D1DR and D2DR MSN output (Francis *et al*, 2014; Kim *et al*, 2011; Lobo *et al*, 2010; MacAskill *et al*, 2014). Indeed, a recent report showed that CIE exposure and withdrawal prevented the induction of low frequency long-term depression (LTD) in D1DR-expressing MSNs and instead led to the occurrence of LTD in D1DR-non-expressing MSNs (Jeanes *et al*, 2014). Although we did not observe any apparent bimodal effects of CIE exposure on $K_{Ca}2$ channel function in the NAc core, it is possible that CIE exposure produces cell-type-specific effects on $K_{Ca}2$ channel function in D1DR and D2DR-expressing MSNs that could drive escalation of drinking in dependent mice. Further studies are needed to address this possibility.

In summary, results of the present study clearly demonstrate that *KCNN1-3* gene expression in the brain is an important factor in alcohol, nicotine, and drug addiction. We validated these clinical and preclinical observations using genetically diverse BXD strains and targeted pharmacological inhibition of $K_{Ca}2$ channels in limited-access and dependence-induced escalation of drinking models. Based on our findings, we propose that human laboratory studies and clinical trials coupled with genetic profiling of heavy drinking alcoholics should be initiated to determine if $K_{Ca}2$ channels are a promising pharmacogenetic target for treating AUDs. Additional studies should also explore the suggestion that $K_{Ca}2$ channels are a possible biomarker for substance

abuse or a pharmacogenetic target for reducing the intake of nicotine and illicit drugs.

FUNDING AND DISCLOSURE

The authors declare no conflict of interest.

ACKNOWLEDGMENTS

The authors would like to thank Jason Emory Parker and Harold (JR) Haun for their technical assistance in the completion of some aspects of these studies. These studies were supported by NIH grants AA020930 (PJM); AA020929 (MFL); AA014095 and AA010761 (HCB); AA018776 (EJC); AA016667 (MFM); AA010761 and AA009986 (JJW); and AA013499 and AA016662 (RWW).

REFERENCES

Adelman JP, Maylie J, Sah P (2012). Small-conductance Ca2+-activated K+ channels: form and function. *Annu Rev Physiol* **74**: 245–269.

Agrawal A, Verweij KJ, Gillespie NA, Heath AC, Lessov-Schlaggar CN, Martin NG *et al* (2012). The genetics of addiction-a translational perspective. *Transl Psychiatry* **2**: e140.

Albertson DN, Schmidt CJ, Kapatos G, Bannon MJ (2006). Distinctive profiles of gene expression in the human nucleus accumbens associated with cocaine and heroin abuse. *Neuropsychopharmacology* **31**: 2304–2312.

Aldridge GM, Podrebarac DM, Greenough WT, Weiler IJ (2008). The use of total protein stains as loading controls: an alternative to high-abundance single-protein controls in semi-quantitative immunoblotting. *J Neurosci Methods* **172**: 250–254.

Anton RF, Oroszi G, O'Malley S, Couper D, Swift R, Pettinati H *et al* (2008). An evaluation of mu-opioid receptor (OPRM1) as a predictor of naltrexone response in the treatment of alcohol dependence: results from the Combined Pharmacotherapies and Behavioral Interventions for Alcohol Dependence (COMBINE) study. *Arch Gen Psychiatry* **65**: 135–144.

Anton RF, Voronin KK, Randall PK, Myrick H, Tiffany A (2012). Naltrexone modification of drinking effects in a subacute treatment and bar-lab paradigm: influence of OPRM1 and dopamine transporter (SLC6A3) genes. *Alcohol Clin Exp Res* **36**: 2000–2007.

Baker EJ, Jay JJ, Bubier JA, Langston MA, Chesler EJ (2012). GeneWeaver: a web-based system for integrative functional genomics. *Nucleic Acids Res* **40**(Database issue): D1067–D1076.

Becker HC, Lopez MF (2004). Increased ethanol drinking after repeated chronic ethanol exposure and withdrawal experience in C57BL/6 mice. *Alcohol Clin Exp Res* **28**: 1829–1838.

Bond CT, Herson PS, Strassmaier T, Hammond R, Stackman R, Maylie J *et al* (2004). Small conductance Ca2+-activated K+ channel knock-out mice reveal the identity of calcium-dependent afterhyperpolarization currents. *J Neurosci* **24**: 5301–5306.

Bowen T, Williams N, Norton N, Spurlock G, Wittekindt OH, Morris-Rosendahl DJ *et al* (2001). Mutation screening of the KCNN3 gene reveals a rare frameshift mutation. *Mol Psychiatry* **6**: 259–260.

Chandy KG, Fantino E, Wittekindt O, Kalman K, Tong LL, Ho TH *et al* (1998). Isolation of a novel potassium channel gene hSKCa3 containing a polymorphic CAG repeat: a candidate for schizophrenia and bipolar disorder? *Mol Psychiatry* **3**: 32–37.

Crettol S, Deglon JJ, Besson J, Croquette-Krokar M, Hammig R, Gothuey I *et al* (2006). ABCB1 and cytochrome P450 genotypes and phenotypes: influence on methadone plasma levels and response to treatment. *Clin Pharmacol Ther* **80**: 668–681.

Crettol S, Deglon JJ, Besson J, Croquette-Krokkar M, Gothuey I, Hammig R *et al* (2005). Methadone enantiomer plasma levels, CYP2B6, CYP2C19, and CYP2C9 genotypes, and response to treatment. *Clin Pharmacol Ther* **78**: 593–604.

Deignan J, Lujan R, Bond C, Riegel A, Watanabe M, Williams JT *et al* (2012). SK2 and SK3 expression differentially affect firing frequency and precision in dopamine neurons. *Neuroscience* **217**: 67–76.

Deschaux O, Bizot JC, Goyffon M (1997). Apamin improves learning in an object recognition task in rats. *Neurosci Lett* **222**: 159–162.

Dittmer A, Dittmer J (2006). Beta-actin is not a reliable loading control in western blot analysis. *Electrophoresis* **27**: 2844–2845.

Fonseca F, de la Torre R, Diaz L, Pastor A, Cuyas E, Pizarro N *et al* (2011). Contribution of cytochrome P450 and ABCB1 genetic variability on methadone pharmacokinetics, dose requirements, and response. *PLoS One* **6**: e19527.

Francis TC, Chandra R, Friend DM, Finkel E, Dayrit G, Miranda J *et al* (2014). Nucleus accumbens medium spiny neuron subtypes mediate depression-related outcomes to social defeat stress. *Biol Psychiatry* **77**: 212–222.

Grice DE, Reenila I, Mannisto PT, Brooks AI, Smith GG, Golden GT *et al* (2007). Transcriptional profiling of C57 and DBA strains of mice in the absence and presence of morphine. *BMC Genomics* **8**: 76.

Griffin WC 3rd, Haun HL, Hazelbaker CL, Ramachandra VS, Becker HC (2014). Increased extracellular glutamate in the nucleus accumbens promotes excessive ethanol drinking in ethanol dependent mice. *Neuropsychopharmacology* **39**: 707–717.

Griffin WC 3rd, Lopez MF, Yanke AB, Middaugh LD, Becker HC (2009). Repeated cycles of chronic intermittent ethanol exposure in mice increases voluntary ethanol drinking and ethanol concentrations in the nucleus accumbens. *Psychopharmacology (Berl)* **201**: 569–580.

Grube S, Gerchen MF, Adamcio B, Pardo LA, Martin S, Malzahn D *et al* (2011). A CAG repeat polymorphism of KCNN3 predicts SK3 channel function and cognitive performance in schizophrenia. *EMBO Mol Med* **3**: 309–319.

Hammond RS, Bond CT, Strassmaier T, Ngo-Anh TJ, Adelman JP, Maylie J *et al* (2006). Small-conductance Ca2+-activated K+ channel type 2 (SK2) modulates hippocampal learning, memory, and synaptic plasticity. *J Neurosci* **26**: 1844–1853.

Heilig M, Goldman D, Berrettini W, O'Brien CP (2011). Pharmacogenetic approaches to the treatment of alcohol addiction. *Nat Rev Neurosci* **12**: 670–684.

Heiman M, Schaefer A, Gong S, Peterson JD, Day M, Ramsey KE *et al* (2008). A translational profiling approach for the molecular characterization of CNS cell types. *Cell* **135**: 738–748.

Herrik KF, Redrobe JP, Holst D, Hougaard C, Sandager-Nielsen K, Nielsen AN *et al* (2012). CyPPA, a positive SK3/SK2 modulator, reduces activity of dopaminergic neurons, inhibits dopamine release, and counteracts hyperdopaminergic behaviors induced by methylphenidate. *Front Pharmacol* **3**: 11.

Hopf FW, Bowers MS, Chang SJ, Chen BT, Martin M, Seif T *et al* (2010). Reduced nucleus accumbens SK channel activity enhances alcohol seeking during abstinence. *Neuron* **65**: 682–694.

Hopf FW, Martin M, Chen BT, Bowers MS, Mohamedi MM, Bonci A (2007). Withdrawal from intermittent ethanol exposure increases probability of burst firing in VTA neurons in vitro. *J Neurophysiol* **98**: 2297–2310.

Hopf FW, Simms JA, Chang SJ, Seif T, Bartlett SE, Bonci A (2011). Chlorzoxazone, an SK-type potassium channel activator used in humans, reduces excessive alcohol intake in rats. *Biol Psychiatry* **69**: 618–624.

Ishikawa M, Mu P, Moyer JT, Wolf JA, Quock RM, Davies NM *et al* (2009). Homeostatic synapse-driven membrane plasticity in nucleus accumbens neurons. *J Neurosci* **29**: 5820–5831.

Jacobsen JP, Weikop P, Hansen HH, Mikkelsen JD, Redrobe JP, Holst D *et al* (2008). SK3 K+ channel-deficient mice have

enhanced dopamine and serotonin release and altered emotional behaviors. *Genes Brain Behav* **7**: 836–848.

Jeanes ZM, Buske TR, Morrisett RA (2014). Cell type-specific synaptic encoding of ethanol exposure in the nucleus accumbens shell. *Neuroscience* **277**: 184–195.

Johnstone EC, Yudkin PL, Hey K, Roberts SJ, Welch SJ, Murphy MF *et al* (2004). Genetic variation in dopaminergic pathways and short-term effectiveness of the nicotine patch. *Pharmacogenetics* **14**: 83–90.

Keeler JF, Pretsell DO, Robbins TW (2014). Functional implications of dopamine D1 vs. D2 receptors: a 'prepare and select' model of the striatal direct vs. indirect pathways. *Neuroscience* **282C**: 156–175.

Kim J, Park BH, Lee JH, Park SK, Kim JH (2011). Cell type-specific alterations in the nucleus accumbens by repeated exposures to cocaine. *Biol Psychiatry* **69**: 1026–1034.

Kohler M, Hirschberg B, Bond CT, Kinzie JM, Marrion NV, Maylie J *et al* (1996). Small-conductance, calcium-activated potassium channels from mammalian brain. *Science* **273**: 1709–1714.

Kranzler HR, McKay JR (2012). Personalized treatment of alcohol dependence. *Curr Psychiatry Rep* **14**: 486–493.

Lerman C, Jepson C, Wileyto EP, Epstein LH, Rukstalis M, Patterson F *et al* (2006). Role of functional genetic variation in the dopamine D2 receptor (DRD2) in response to bupropion and nicotine replacement therapy for tobacco dependence: results of two randomized clinical trials. *Neuropsychopharmacology* **31**: 231–242.

Lobo MK, Covington HE 3rd, Chaudhury D, Friedman AK, Sun H, Damez-Werno D *et al* (2010). Cell type-specific loss of BDNF signaling mimics optogenetic control of cocaine reward. *Science* **330**: 385–390.

Lopez MF, Becker HC (2005). Effect of pattern and number of chronic ethanol exposures on subsequent voluntary ethanol intake in C57BL/6J mice. *Psychopharmacology (Berl)* **181**: 688–696.

MacAskill AF, Cassel JM, Carter AG (2014). Cocaine exposure reorganizes cell type- and input-specific connectivity in the nucleus accumbens. *Nat Neurosci* **17**: 1198–1207.

Mi H, Muruganujan A, Casagrande JT, Thomas PD (2013). Large-scale gene function analysis with the PANTHER classification system. *Nat Protoc* **8**: 1551–1566.

Miller MJ, Rauer H, Tomita H, Rauer H, Gargus JJ, Gutman GA *et al* (2001). Nuclear localization and dominant-negative suppression by a mutant SKCa3 N-terminal channel fragment identified in a patient with schizophrenia. *J Biol Chem* **276**: 27753–27756.

Mu P, Moyer JT, Ishikawa M, Zhang Y, Panksepp J, Sorg BA *et al* (2010). Exposure to cocaine dynamically regulates the intrinsic membrane excitability of nucleus accumbens neurons. *J Neurosci* **30**: 3689–3699.

Mulholland PJ (2012). K(Ca)2 channels: novel therapeutic targets for treating alcohol withdrawal and escalation of alcohol consumption. *Alcohol* **46**: 309–315.

Mulholland PJ, Becker HC, Woodward JJ, Chandler LJ (2011). Small conductance calcium-activated potassium type 2 channels regulate alcohol-associated plasticity of glutamatergic synapses. *Biol Psychiatry* **69**: 625–632.

Ngo-Anh TJ, Bloodgood BL, Lin M, Sabatini BL, Maylie J, Adelman JP (2005). SK channels and NMDA receptors form a Ca2+-mediated feedback loop in dendritic spines. *Nat Neurosci* **8**: 642–649.

Oslin DW, Berrettini W, Kranzler HR, Pettinati H, Gelernter J, Volpicelli JR *et al* (2003). A functional polymorphism of the mu-opioid receptor gene is associated with naltrexone response in alcohol-dependent patients. *Neuropsychopharmacology* **28**: 1546–1552.

Padula A, McGuier N, Griffin W, Lopez M, Becker H, Mulholland P (2013). Novel anticonvulsants for reducing alcohol consumption: a review of evidence from preclinical rodent drinking models. *OA alcohol* **1**: 2.

Ponomarev I, Wang S, Zhang L, Harris RA, Mayfield RD (2012). Gene coexpression networks in human brain identify epigenetic modifications in alcohol dependence. *J Neurosci* **32**: 1884–1897.

Ray LA, Hutchison KE (2007). Effects of naltrexone on alcohol sensitivity and genetic moderators of medication response: a double-blind placebo-controlled study. *Arch Gen Psychiatry* **64**: 1069–1077.

Rhodes JS, Best K, Belknap JK, Finn DA, Crabbe JC (2005). Evaluation of a simple model of ethanol drinking to intoxication in C57BL/6J mice. *Physiol Behav* **84**: 53–63.

Sailer CA, Hu H, Kaufmann WA, Trieb M, Schwarzer C, Storm JF *et al* (2002). Regional differences in distribution and functional expression of small-conductance Ca2+-activated K+ channels in rat brain. *J Neurosci* **22**: 9698–9707.

Sailer CA, Kaufmann WA, Marksteiner J, Knaus HG (2004). Comparative immunohistochemical distribution of three small-conductance Ca2+-activated potassium channel subunits, SK1, SK2, and SK3 in mouse brain. *Mol Cell Neurosci* **26**: 458–469.

Schacht JP, Anton RF, Voronin KE, Randall PK, Li X, Henderson S *et al* (2013). Interacting effects of naltrexone and OPRM1 and DAT1 variation on the neural response to alcohol cues. *Neuropsychopharmacology* **38**: 414–422.

Soden ME, Jones GL, Sanford CA, Chung AS, Guler AD, Chavkin C *et al* (2013). Disruption of dopamine neuron activity pattern regulation through selective expression of a human KCNN3 mutation. *Neuron* **80**: 997–1009.

Sturgess JE, George TP, Kennedy JL, Heinz A, Muller DJ (2011). Pharmacogenetics of alcohol, nicotine and drug addiction treatments. *Addict Biol* **16**: 357–376.

Swan GE, Valdes AM, Ring HZ, Khroyan TV, Jack LM, Ton CC *et al* (2005). Dopamine receptor DRD2 genotype and smoking cessation outcome following treatment with bupropion SR. *Pharmacogenomics J* **5**: 21–29.

Uhl GR, Liu QR, Drgon T, Johnson C, Walther D, Rose JE *et al* (2008). Molecular genetics of successful smoking cessation: convergent genome-wide association study results. *Arch Gen Psychiatry* **65**: 683–693.

Wang J, Gutala R, Hwang YY, Kim JM, Konu O, Ma JZ *et al* (2008). Strain- and region-specific gene expression profiles in mouse brain in response to chronic nicotine treatment. *Genes Brain Behav* **7**: 78–87.

Welinder C, Ekblad L (2011). Coomassie staining as loading control in western blot analysis. *J Proteome Res* **10**: 1416–1419.

Whiteford HA, Degenhardt L, Rehm J, Baxter AJ, Ferrari AJ, Erskine HE *et al* (2013). Global burden of disease attributable to mental and substance use disorders: findings from the Global Burden of Disease Study 2010. *Lancet* **382**: 1575–1586.

Wolen AR, Phillips CA, Langston MA, Putman AH, Vorster PJ, Bruce NA *et al* (2012). Genetic dissection of acute ethanol responsive gene networks in prefrontal cortex: functional and mechanistic implications. *PLoS One* **7**: e33575.

Wolfart J, Neuhoff H, Franz O, Roeper J (2001). Differential expression of the small-conductance, calcium-activated potassium channel SK3 is critical for pacemaker control in dopaminergic midbrain neurons. *J Neurosci* **21**: 3443–3456.

Woltman H, Feldstain A, MacKay JC, Rocchi M (2012). An introduction to hierarchical linear modeling. *Tutorials Quant Methods Psychology* **8**: 52–69.

Supplementary Information accompanies the paper on the Neuropsychopharmacology website (http://www.nature.com/npp)